JOURNAL OF CATALYSIS 83, 192–204 (1983)

Conversion of Methanol into Hydrocarbons over Ammonium 12-Tungstophosphate

H. HAYASHI[1] AND J. B. MOFFAT[2]

Department of Chemistry and Guelph-Waterloo Center for Graduate Work in Chemistry, University of Waterloo, Waterloo, Ontario, Canada N2L 3G1

Received May 21, 1983; revised February 18, 1983

The ammonium salt of 12-tungstophosphoric acid has been prepared and characterized through powder X-ray diffraction, acid strength, chemisorption of ammonia, and thermal and chemical analyses. The adsorptive and cracking properties of the salt with respect to olefins and paraffins has also been examined. The ammonium salt is found to have a considerably higher catalytic activity for the conversion of methanol to hydrocarbons than that of any other heteropoly compounds reported previously. In addition, in contrast to the observations with other heteropoly compounds, the ammonium salt displays a high selectivity for the formation of saturated hydrocarbons rather than olefins.

INTRODUCTION

In recent years solids with surface acidic functionalities and containing three or more elements in the anionic component have received increasing attention as heterogeneous catalysts. One such group of substances, often referred to as heteropoly acids, possesses complex and high molecular weight anions with 2 to 18 hexavalent molybdenum or tungsten, or pentavalent vanadium or niobium atoms around one or more central atoms (*1*). The central atoms are commonly P, Ni, As, Te, and Mn, although approximately 36 different elements have been employed in this capacity in various heteropoly anions (*1*). Heteropoly compounds in general (*1*) and heteropoly compounds of molybdenum and tungsten (*2*) have recently been reviewed by Tsigdinos.

Fortunately, X-ray structure analyses are available on many of the heteropoly compounds. For example, in the 12-tungstophosphate anions $[PW_{12}O_{40}]^{3-}$, each tungsten atom is at the center of an octahedron and each oxygen atom is situated at each vertex. Tsigdinos (*1*) has noted that these octahedra may be considerably distorted. The phosphorus atom is located at the center of a PO_4 tetrahedron which is itself surrounded by WO_6 octahedra which share corners and edges to produce the Keggin structure (Fig. 1).

The earlier work on the catalytic properties of heteropoly compounds began to appear as recently as 1978 and was primarily concerned with the heteropoly acids $H_3PX_{12}O_{40}$ where X is Mo or W. The earlier catalytic studies have been recently reviewed (*3a*). More recently, reports on the catalytic properties of the salts of these heteropoly acids have appeared (*3–9*). The structure and acidity of 12-molybdophosphoric acid and its salts have been studied with the use of infrared spectroscopy (*4*). The vapor-phase oxidation of a number of compounds has been examined with a variety of salts of 12-molybdophosphoric acid (*5–7*). The *O*-alkylation of $[PMo_{12}O_{40}]^{3-}$ and $[PW_{12}O_{40}]^{3-}$ has been reported (*8*). Alkali and alkaline-earth salts of the 12-heteropolymolybdates with P, As, or Si as the heteroatoms have been shown to be effective in the vapor-phase oxidative dehydrogenation of isobutyric acid (*9*).

---

[1] On leave from Dept. of Chemical Engineering, Tokushima University, Minamijosanjima, Tokushima, 770 Japan.

[2] To whom correspondence should be addressed.

0021-9517/83 $3.00

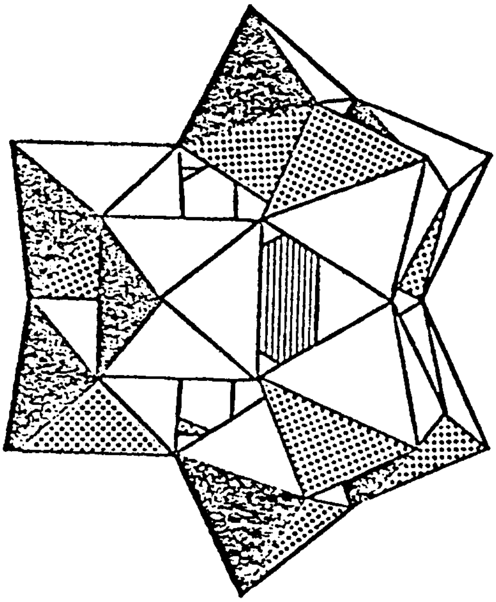

FIG. 1. Polyhedral diagram of 12-tungstophosphate anion $[PW_{12}O_{40}]^{3-}$.

The conversion of methanol to hydrocarbons over copper and silver salts of 12-tungstophosphoric acid and 12-tungstosilicic acid has been reported (*10, 11*).

In spite of the current interest in the catalytic properties of the heteropoly acids and their salts, relatively little work has been reported on organic salts of these acids. After the present work was complete a report on the selective formation of ethylene and propylene from methanol over pyrazinium salts of 12-tungstophosphoric acid appeared (*12*).

The present report describes the preparation, characterization, and catalytic properties of ammonium 12-tungstophosphate. The conversion of methanol to hydrocarbons and the cracking of hydrocarbons have been employed as the principal reactions of interest. This work results primarily from an extension of earlier work on the conversion of methanol to hydrocarbons on the heteropoly acids, 12-molybdophosphoric acid, 12-tungstophosphoric acid, the dimeric 9-tungstophosphoric acid (*3a*), and the metal salts of 12-tungstophosphoric acid (*3c*).

EXPERIMENTAL

Apparatus and Procedure

Reactions of methanol and hydrocarbons were carried out in a microcatalytic pulse reactor described in the previous paper (*3a*). Adsorption studies of hydrocarbons were performed with the same apparatus, where the catalyst column was directly connected with the detector.

Materials

Ammonium 12-tungstophosphate precipitated immediately by the stepwise addition of the stoichiometric amount of ammonium carbonate (Baker Analyzed Reagent) into an aqueous solution of 12-tungstophosphoric acid (BDH Chemicals, AnalaR grade). The milky-white colloidal solution was concentrated over a boiling-water bath. The resultant paste was spread over a Petri dish and dried overnight at room temperature to give $(NH_4)_3PW_{12}O_{40} \cdot 8H_2O$. Phosphorus content (*3b*)—*Anal.* Calcd for 8-hydrate: 0.325_2 mg-atom/g. Found: 0.324_5 mg-atom/g. Methanol and liquid hydrocarbons were obtained from Baker Chemicals. Dimethyl ether and gaseous hydrocarbons were obtained from Matheson as CP grade in lecture bottles. All chemicals and gases were used as received.

Characterization of Catalyst

Powder X-ray diffraction, acid strength by the indicator method, and chemisorption of ammonia were employed as means of characterization of the catalysts. The powder X-ray diffraction data were obtained with a Phillips diffractometer (model PW-1011/60) at 40 kV and 30 mA with Cu$K\alpha$ radiation. Acid strength was determined with the following indicators (pKa): benzeneazodiphenylamine (+1.5), dicinnamalacetone (−3.0), benzalacetophenone (−5.6), and anthraquinone (−8.2). The total number of acidic sites was estimated from the chemisorption of ammonia at room temperature using a quartz-spring balance. An aliquot of sample was evacuated overnight,

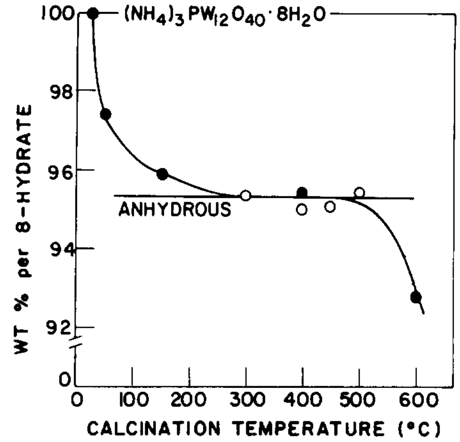

FIG. 2. Weight decrease in calcination of $(NH_4)_3PW_{12}O_{40} \cdot 8H_2O$. ●: calcined in air for 2 hr, ○: calcined in helium for 2 hr.

equilibrated under 390–400 Torr ammonia, and again evacuated overnight to a constant weight. BET areas were measured by nitrogen adsorption at liquid-nitrogen temperature using a quartz-spring balance. Chemical composition of catalysts was determined by EDTA (*3b*) for phosphorus and tungsten. Nitrogen content was analyzed by M-H-W Laboratories, Phoenix.

RESULTS

Thermal Properties of Ammonium 12-Tungstophosphate

The results for thermogravimetry of $(NH_4)_3PW_{12}O_4 \cdot 8H_2O$ are shown in Fig. 2. The weight decreased to a constant value at approximately 300°C and remained constant up to 500°C. The nitrogen content of 1.42 wt% for the salt calcined at 400°C in air for 2 hr agreed well with that of 1.43 wt% calculated for anhydrous $(NH_4)_3PW_{12}O_{40}$. Thus the plateau observed between 300 and 500°C can be associated with the formation of the anhydrous salt. Further heating of the salt but at 600°C produced a substantial decrease in weight and a color change from white to dark green. Since the phosphorus content decreased to 55% per Keggin unit at 600°C, the loss in weight may be attributed to the sublimation of P_2O_5 as found with the free acid (*3a*).

Figure 3 shows powder X-ray data for the ammonium salt in comparison with the free acid. The gross features of the diffraction pattern are similar for the acid and the salt, but a small shift in the 2θ values is evident. A comparison of the data for the hydrated ammonium salt with that for the anhydrous salt obtained after heating in helium at 450°C for 2 hr confirms the retention of the heteropoly structure. The decomposition product from $(NH_4)_3PW_{12}O_{40}$ at 600°C showed a pattern similar to that of $H_3PW_{12}O_{40}$.

Surface Area and Acidic Properties

The variation of the surface area of the ammonium salt with calcination temperature is illustrated in Fig. 4. Calcination at 400°C in helium and in air gave essentially the same area of 113 and 112 m^2/g, respectively. On heating in helium to 300°C the surface area reaches a maximum of 163 m^2/g and subsequently decreases monotonically with further heating to 600°C. In contrast the surface area of $H_3PW_{12}O_{40}$ (*3a*) and its metal salts (*3c*) calcined at 400°C in helium was measured as 3–6 m^2/g.

Hammett indicators showed the presence of surface sites on both the free acid and ammonium salt with pKa as low as −8.2. Evidently the acidity of at least some of the sites on the salt is as high as that of the parent acid.

The total amount of acidic sites estimated from the chemisorption of ammonia is also given in Fig. 4. The quantity of ammonia chemisorbed increases with calcination temperature, reaches a maximum at approximately 400°C, and subsequently decreases with further increase in temperature. The amount of ammonia chemisorbed on $H_3PW_{12}O_{40}$ calcined at 300–450°C in helium was 1.48–1.62 mmole/g, somewhat higher than the 1.0_4 mmole/g expected as tribasic acid (*3a*). The values of 0.53–0.59 mmole/g given in Fig. 4 for $(NH_4)_3PW_{12}O_{40}$ calcined at 300–400°C may account for the above discrepancy. The surface concentration of acidic sites on $(NH_4)_3PW_{12}O_{40}$ of

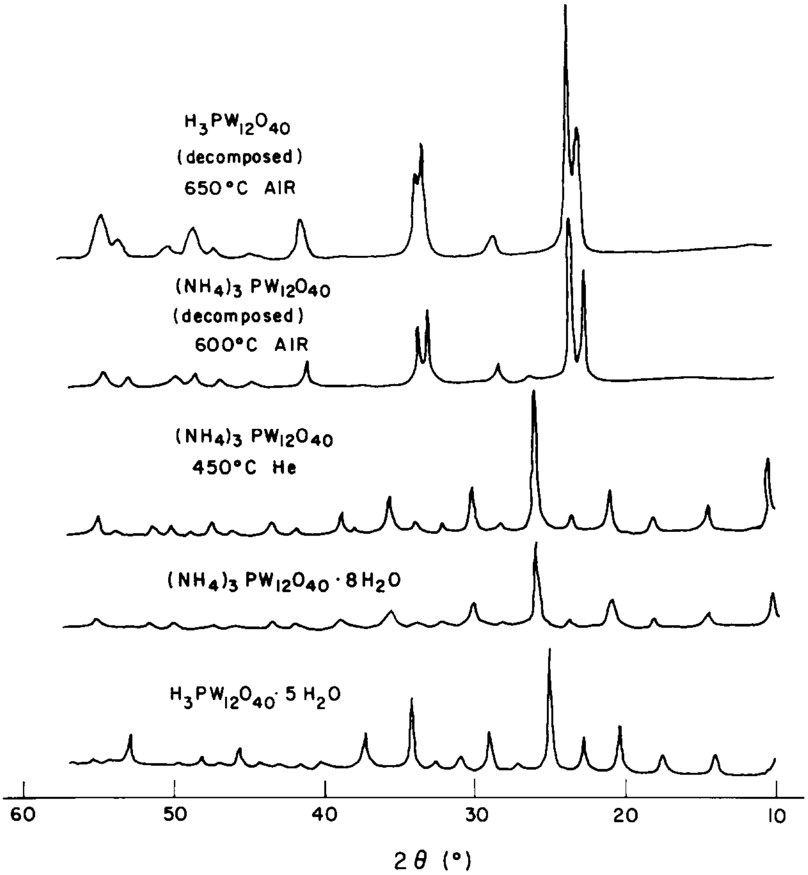

FIG. 3. Powder X-ray patterns for $(NH_4)_3PW_{12}O_{40}$ and $H_3PW_{12}O_{40}$ calcined at various conditions.

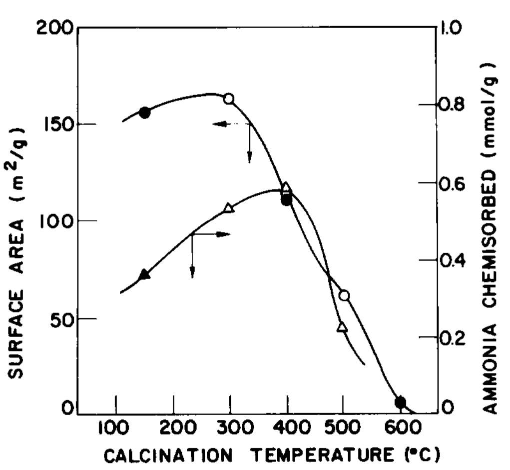

FIG. 4. Effect of calcination temperature on the surface area and acidity of $(NH_4)_3PW_{12}O_{40}$. Black symbols: calcined in air, white symbols: calcined in helium.

1.9_5–$3.1_3 \times 10^{14}$ meq/cm² compares closely with data reported in the literature on other acidic catalysts. Surface densities of hydroxyl groups of between 1.5×10^{14} and 4.5×10^{14} molecules/cm² have been reported for silica catalysts (*13, 14*), while 1.2–7.5×10^{14} hydrogen atoms/cm² have been found on boron phosphate (*15*).

Adsorption of ammonia decreased the acid strength of $(NH_4)_3PW_{12}O_{40}$, which was, however, still acidic at +1.5 for pKa.

Adsorption Behavior of Hydrocarbons

A substantial difference was observed in the chromatographic adsorption behavior of hydrocarbons on $H_3PW_{12}O_{40}$ and $(NH_4)_3PW_{12}O_{40}$ at lower temperatures. Propylene and butenes were trapped irrevers-

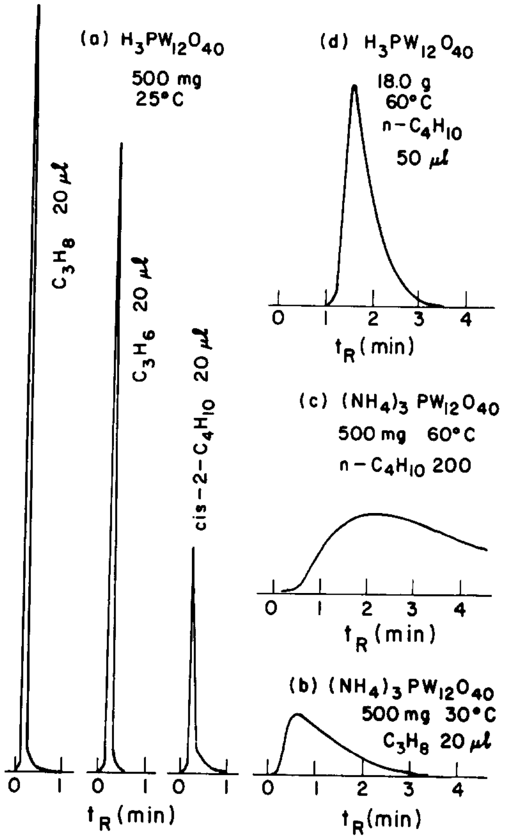

FIG. 5. Chromatographic adsorption behavior of hydrocarbons on $H_3PW_{12}O_{40}$ and $(NH_4)_3PW_{12}O_{40}$. Carrier gas: He, 30 ml/min; catalysts: calcined at 400°C in helium.

ibly on the ammonium salt, while partly reversible on the free acid as shown in Fig. 5(a). Adsorption of propane (b) and *n*-butane (c) on $(NH_4)_3PW_{12}O_{40}$ was reversible, but the eluted peaks were quite broad in comparison with $H_3PW_{12}O_{40}$ (a). The difference in the adsorption behavior might arise partly from that in surface area, the values of which were 113 and 3.1 m^2/g by BET for $(NH_4)_3PW_{12}O_{40}$ and $H_3PW_{12}O_{40}$, respectively. To eliminate the effect of such differences in area, a comparison was made for *n*-butane at 60°C using 500 mg of $(NH_4)_3PW_{12}O_{40}$ (c) and 18.0 g of $H_3PW_{12}O_{40}$ (d) with an equal area of 56 m^2/adsorbent. The retention times were close together as expected, but the peak was still broader for $(NH_4)_3PW_{12}O_{40}$. Heats of adsorption evaluated from the temperature dependency of retention times for C_3H_8, *n*-C_4H_{10} and *n*-C_5H_{12} on $(NH_4)_3PW_{12}O_{40}$ were 6.2, 7.8, and 9.1 kcal/mole, respectively. These values are within the range of values usually associated with physical adsorption.

Methanol to Hydrocarbons

As can be observed from Figs. 6–9, $(NH_4)_3PW_{12}O_{40}$ is an efficient catalyst for methanol conversion into hydrocarbons.

Figure 6 compares the effects of reaction temperature on the methanol conversion over $H_3PW_{12}O_{40}$ (a) and $(NH_4)_3PW_{12}O_{40}$ (b) both calcined at 400°C in helium. The results show higher yields of hydrocarbons for the ammonium salt than for the free acid. The total yield of C_1–C_5 hydrocarbons was 76.9% for $(NH_4)_3PW_{12}O_{40}$ at 350°C,

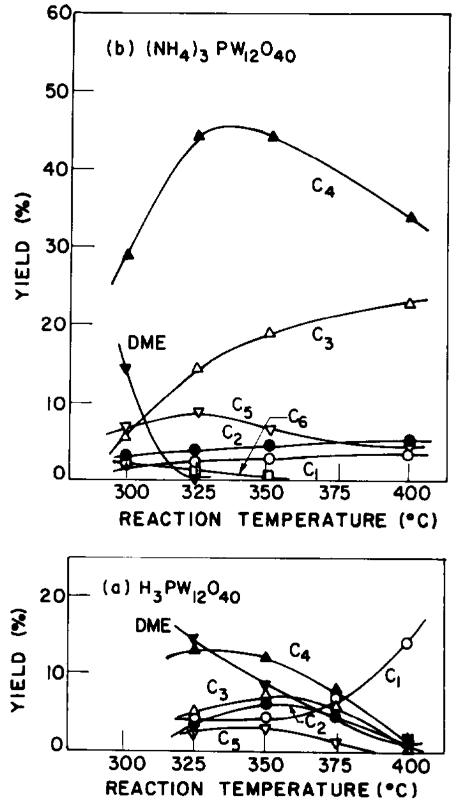

FIG. 6. Effect of reaction temperature on the methanol conversion over $H_3PW_{12}O_{40}$ (a) and $(NH_4)_3PW_{12}O_{40}$ (b). Catalysts: calcined at 400°C in helium for 2 hr; *W*/*F* = 246 mg-cat min/ml-He.

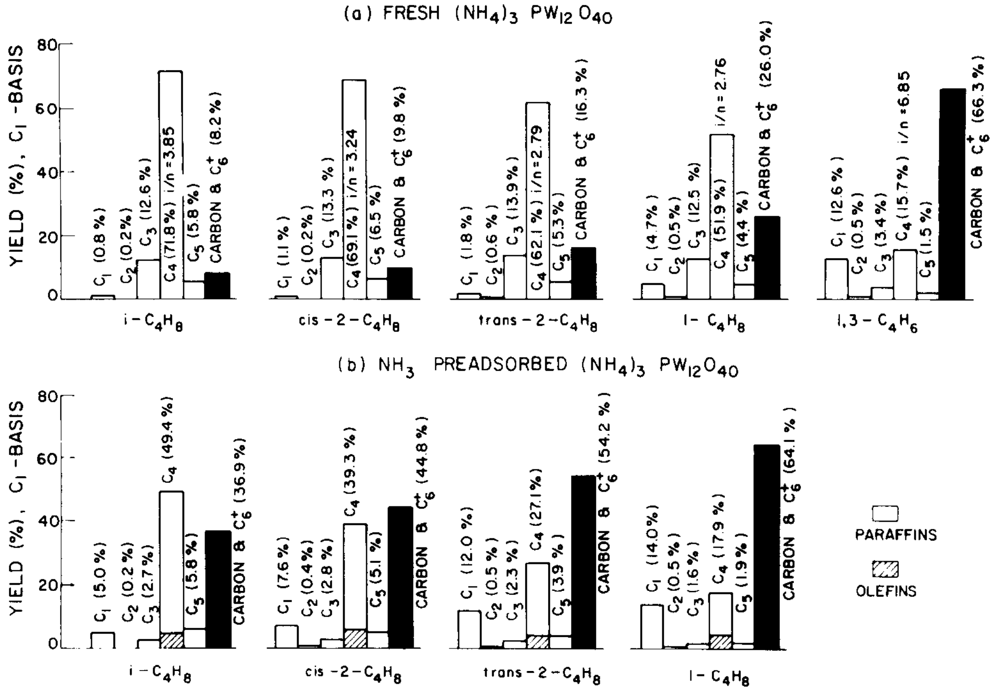

FIG. 7. Product distributions in the cracking of butenes on fresh (a) and NH_3 preadsorbed (b) $(NH_4)_3PW_{12}O_{40}$. Reaction: 350°C, W/F = 250 mg-cat min/ml-He; catalysts: (a) calcined at 400°C in air for 2 hr, (b) Gaseous NH_3 was passed at room temperature for 1 hr and then calcined at 400°C in air for 2 hr.

while that for $H_3PW_{12}O_{40}$ was 32.4%, showing higher carbonization on the more strongly acidic free acid. It is of interest that the hydrocarbons produced on the ammonium salt were paraffinic except for a small amount of ethylene (yield 2.0–2.8%). The major product was butanes, in which the iso content was 86.5, 80.7, and 75.9% at 325, 350, and 400°C, respectively. The maximum in yield seems to shift toward lower temperature as the carbon number increases. In contrast, olefins were detected for $H_3PW_{12}O_{40}$.

Figure 7 gives further information about hydrocarbon behavior on the fresh (a) and the ammonia preadsorbed (b) ammonium salt. Hydrocarbon yield on the fresh catalyst (a) increased in the order of *i*-C_4, *cis*-2-C_4, *trans*-2-C_4, 1-C_4, 1,3-C_4. The highest yield of hydrocarbons from isobutene and substantial carbonization for 1,3-butadiene are quite reasonable. However, the three straight-chain monoolefins showed some differences in the hydrocarbon yield, while they should presumably produce the same carbonium ion.

Adsorption of ammonia on $(NH_4)_3PW_{12}O_{40}$ decreased the acid strength as previously mentioned, and resulted in the complete deactivation of the catalyst in the methanol conversion into hydrocarbons. Dimethyl ether was obtained in a high yield, but no hydrocarbons were detected. However, butenes gave paraffinic products on the ammonia preadsorbed $(NH_4)_3PW_{12}O_{40}$ as shown in Fig. 7(b). The amounts of carbon and C_6^+ increased in parallel with methane as compared with the fresh catalyst (a), but the catalyst was still active for the conversion of butenes and the order of reactivity was again *i*-C_4, *cis*-2-C_4, *trans*-2-C_4, 1-C_4. In contrast with the fresh catalyst a mixture of butenes was obtained, suggesting the hydride transfer to afford paraffins was suppressed by the preadsorption of ammonia.

Figure 8 shows the effect of calcination conditions and residence times on the yields of various hydrocarbons from methanol conversion of $(NH_4)_3PW_{12}O_{40}$. The shapes of the four graphs shown in Fig. 8 are generally similar, in contrast to the observation with air-calcined $H_3PW_{12}O_{40}$, where a considerable decrease in hydrocarbon yield was found (*3a*). In all cases shown for the ammonium salt in Fig. 8, the yield of hydrocarbons increases with carbon number to a maximum for C_4 and subsequently decreases for C_5. The yields of each hydrocarbon also show an increase with the apparent residence time (*W/F*) to a maximum at approximately 200 for *W/F*, followed by a decrease with further increase in *W/F*. This latter observation applies to air and hydrogen calcination at 400°C (b,c) and helium calcination at 500°C (d). With the catalyst calcined in helium at 400°C, the yields of C_3 and C_4 show little or no evidence of achieving a maximum in the range of *W/F* values employed.

It should also be noted that no color change was observed for the ammonium salt after calcination under hydrogen, but the hydrocarbon yields (c) are somewhat

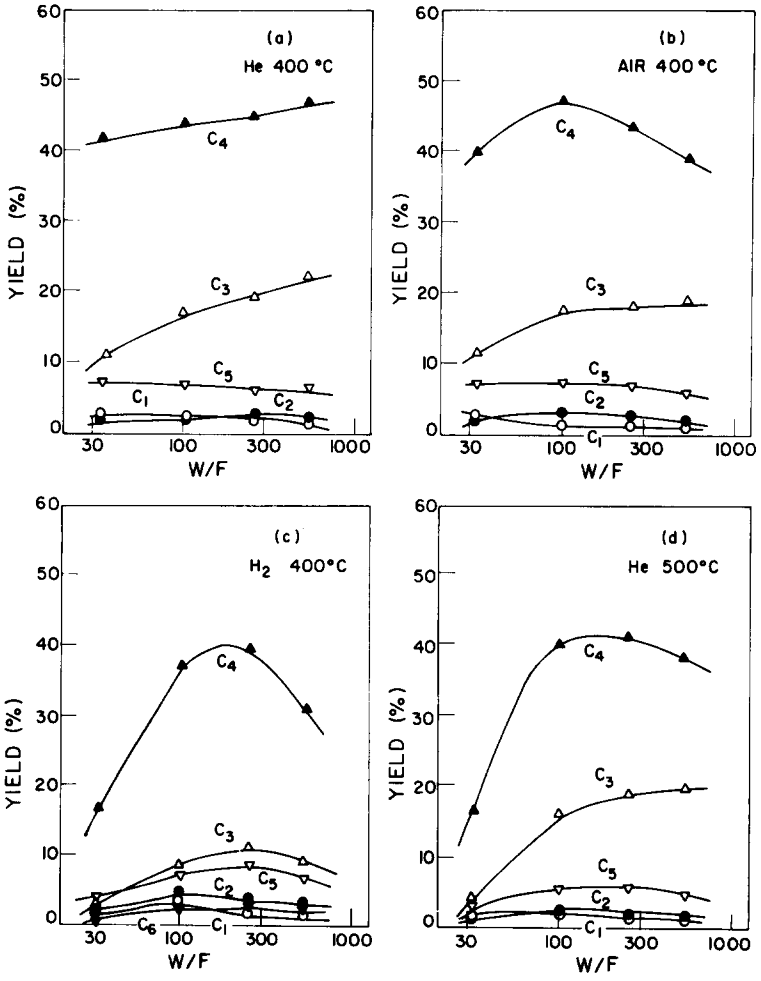

FIG. 8. Effect of calcination conditions in the methanol conversion over $(NH_4)_3PW_{12}O_{40}$. Reaction temperature: 350°C, *W/F* in mg-cat min/ml-He.

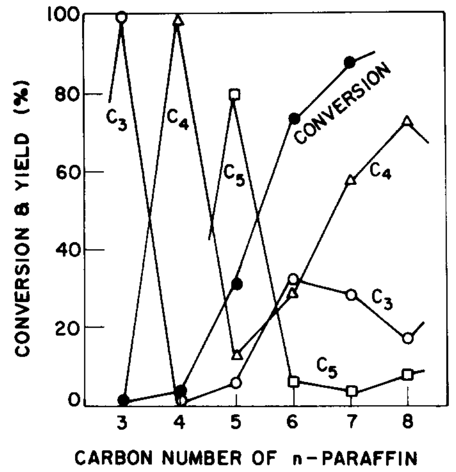

FIG. 9. Cracking behavior of *n*-paraffins over $(NH_4)_3PW_{12}O_{40}$. Catalyst: calcined at 500°C in helium; reaction: 350°C, W/F = 248 mg-cat min/ml-He.

lower than found with this salt after helium or air calcination (a,b) at the same temperature. This is also to be contrasted with the results obtained with the parent heteropoly acid where a color change from white to black, reduction of tungsten (WO_3 to $WO_{2.85}$), and some improvement in hydrocarbon yield were noted after calcination under hydrogen at 400°C (3a).

Calcination of the ammonium salt in helium at a higher temperature of 500°C resulted in a decrease of surface area (Fig. 4), but the activity was largely unchanged as evident from Fig. 8(d).

Cracking Hydrocarbons

As the catalyst is strongly acidic, it seemed likely that cracking of longer-chain hydrocarbons rapidly formed on the surface was involved in the methanol conversion as a possible route to afford C_3–C_5 hydrocarbons as well as carbon-chain propagation starting from C_1 and/or C_2 species (*3a*).

Figure 9 shows the cracking behavior of *n*-paraffins over $(NH_4)_3PW_{12}O_{40}$ at 350°C. Propane was recovered intact. *n*-Butane gave 0.7% C_3 and 1.8% *i*-C_4, but the remainder was recovered as *n*-C_4. Conversion of *n*-paraffins increased rapidly with the increase in the carbon number. All of the products were paraffinic and isobutane was the main product (i/n = 3.0–3.7 in C_4) from higher paraffins, with the production of C_4 paralleling the conversion. The yield of propane and butanes showed maxima at *n*-C_6 and *n*-C_8, respectively. Propane and butanes were obtained also from *n*-C_7 in comparable yield from *n*-C_6 and *n*-C_8. It is of interest to note that the relative amounts of hydrocarbons C_3, C_4, and C_5 from C_6 and C_7 are quite similar to those obtained from methanol.

Figure 10 shows the products from olefins. The product yields from C_3- and C_4-olefins are close to those from C_6- and C_8-paraffins given in Fig. 9, respectively, suggesting a rapid dimerization prior to the cracking reaction. No olefins were detected except ethylene, and isobutane was again the main product (i/n = 4.0–5.3 in C_4). As previously shown in Fig. 5, adsorption of olefins on $(NH_4)_3PW_{12}O_{40}$ was irreversible, while reversible for paraffins. Thus the results in Figs. 9 and 10 suggest the rapid oligomerization of lower olefins strongly trapped on the surface and the subsequent cracking through carbonium ion mechanism with hydride transfer (*16, 17*) to afford lower paraffins. The product patterns

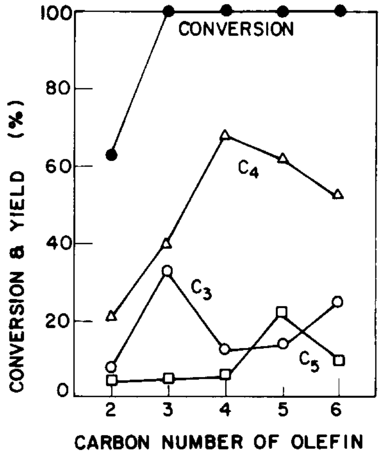

FIG. 10. Products from olefins over $(NH_4)_3PW_{12}O_{40}$. Catalyst and conditions: same as Fig. 9. C_4: *cis*-2-butene; C_5 & C_6: 1-olefin.

are again similar to those found with methanol.

DISCUSSION

The ammonium salt of 12-tungstophosphoric acid possesses some unexpected differences and similarities in properties when compared to those of its parent acid (*3a*). The anhydrous form of the salt appears to be stable over a range of 200° from 300 to approximately 500°C, whereas the anhydrous acid is not obtained until 400°C and decomposes at 500°C. It is evident from the X-ray diffraction data that there is a similarity between the patterns obtained for the free acid and the salt as well as the decomposition products obtained from each. In this regard it should be pointed out that the X-ray diffraction patterns obtained for the sodium, boron, and zirconium salts of 12-tungstophosphoric acid are also similar to each other (*3c*) and to that of the ammonium salt.

The surface area of the ammonium salt is significantly higher than that of the acid. With the salt, the area increases slightly on heating to 300°C. With further heating the surface area decreases monotonically to approximately 5 m^2/g at 600°C.

The quantities of ammonia chemisorbed, either per unit mass or per unit area, both display a maximum at a calcination temperature of approximately 400°C. The maximum acidic strength of sites on both the acid and the ammonium salt is as low as −8.2 (pKa). However, the amounts of ammonia chemisorbed on the salt were approximately one-third of those found with the acid. Thus it appears that the acidic site distribution as a function of strength is much more suppressed in the case of the salt than with the acid. Presumably this may be interpreted as implying that the number of strongly acidic sites on the salt is proportionately reduced relative to these on the acid. It should be emphasized that the ammonium salt was prepared from the free acid with the stoichiometric quantity of ammonium carbonate. While the catalytic behaviour observed with different lots of preparations is reproducible, this does not, of course, preclude the possibility that free protons may be present. Further, the stability of the ammonium salt is demonstrated by the agreement of the measured and the calculated nitrogen contents found for the salt after calcination at 400°C in air for 2 hr. It should be noted, in addition, that attempts to prepare the ammonium salt by chemisorption of ammonia on the acid produced a product with little or no catalytic activity.

The ammonium salt evidently is capable of strongly chemisorbing hydrocarbon species possessing an unsaturated linkage while not chemisorbing saturated species. This suggests that the olefinic species may be interacting with the surface either through π-bonding or as a result of the scission of the double bond to form a single bond and accumulated electron densities at the terminal carbon atoms of the resulting bond. Since the chemisorptive energies with π-bonding are usually considerably smaller than those resulting from the partial cleavage of a bond, the process is more likely to involve the formation of a single bond from the double bond. Although quantitative conclusions are not possible it should be noted that with the ammonium salt the broad peaks generated by saturated hydrocarbons in chromatographic adsorption could be indicative of interparticle and/or intraparticle diffusional resistances.

The total yield of hydrocarbons from methanol between 300 and 400°C is significantly greater on the ammonium salt than on the acid (Fig. 6). However, the pattern of product composition is approximately the same in the two cases. For example, with both catalysts, C_4 hydrocarbons predominate in the product, and these hydrocarbons appear in maximum yield near 350°C. Even more striking, however, is the difference in the nature of the products. The ammonium salt produces primarily saturated hydrocarbons, while the product with the acid is largely olefinic. Although this is consistent with the observations of the differences in adsorptive properties of the salt and free acid, a direct relationship does not necessarily follow. As is discussed later, hydrogen transfer effects are undoubtedly of importance.

The atmosphere in which calcination of the ammonium salt is performed is apparently relatively unimportant. Product patterns from catalysts calcined in helium or air at 400°C are similar although a maximum is evident with the C_4 yield in the latter case. With calcination in hydrogen the C_3 yields are reduced by a factor of approximately two and the C_4 yield is slightly suppressed in comparison with the calcination in helium and air, but no visible evidence of reduction of the ammonium salt was found. Of course calcination in any atmosphere at temperatures greater than 550–600°C will result in significant decomposition of the anionic component of the salt.

The results from the studies of the cracking of hydrocarbons over the ammonium salt are highly reminiscent of results obtained by other workers on a variety of acidic catalysts (*18–24*). It is instructive to note that the equilibrium ratio of *i*-butane to *n*-butane at 350°C is 0.67 (*20*) as compared to approximately 3.0–4.0 in the present work. That such high values can be obtained catalytically has been known for many years (*18–24*). For example, with SiO_2–ZrO_2–Al_2O_3 at 500°C the $i\text{-}C_4/n\text{-}C_4$ ratio was found to be 3.56 (*19*) while more recently a value of 3.33 has been reported for ZSM-5 catalysts at 371°C (*21*). The maximum in the product pattern at C_4 is also not uncommon. For example, as early as 1949, such a C_4-centered product distribution was observed for octane on SiO_2–ZrO_2–Al_2O_3 (*19*). The s-shaped curve observed for the conversion of *n*-paraffins versus carbon number (Fig. 9) was first noted by Greensfelder in 1945 (*18*).

It is apparent from the results presented here that ammonium 12-tungstophosphate is functioning as a acidic catalyst. The product distributions from both the conversion of methanol and of hydrocarbons themselves are suggestive of a predominantly carbonium ion mechanism. Although water is one of the products from the conversion of methanol to hydrocarbons, it does not appear to act as a poison and thus it may be concluded that the active sites are predominantly Brönsted in nature.

As with the parent heteropoly acid itself hydrocarbons begin to form as the dimethyl ether decreases in concentration. The formation of hydrocarbons apparently occurs through the ether as precursor rather than the alcohol. Unlike the parent heteropoly acids, however, no marked increase in the concentration of methane is observed as the concentrations of the higher hydrocarbons pass through their maxima with residence time. In the case of the ammonium salt the concentration of methane either increases only slightly under such conditions or actually decreases. Thus the decrease in concentrations of hydrocarbons with increasing *W*/*F*, at higher residence times may be associated with an irreversible chemisorption of one or more precursors to such hydrocarbons, but without subsequent production of methane.

The relative insensitivity of the ammonium salt to calcination environments and temperatures is consistent with a distribution of acidic strengths in which less strongly acidic sites are favored over the more highly acidic centers. Protons associated with the former are more tightly bound and consequently less susceptible to removal by either reaction or elevated temperatures.

The formation of saturated hydrocarbons virtually to the exclusion of olefinic species is a feature of the conversion of methanol over the ammonium salt and deserves further comment. It may be recalled that it is now generally accepted that zeolites have broad distributions of acidic strengths (*22*), whereas silica–alumina has only very strongly acidic sites. Further, zeolites produce smaller amounts of coke and larger quantities of both aromatics and paraffins in

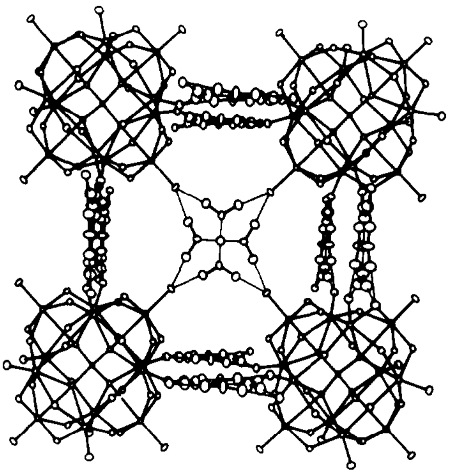

FIG. 11. Stereoscopic drawings showing the packing of anions and diaquahydrogen ions. Reproduced, with permission, from (*25*).

cracking processes than are observed with silica–alumina (*23, 24*). Such differences in behavior have been attributed to relatively higher rates of hydrogen transfer between cracked product molecules with the zeolites as compared to silica–alumina. Although the comparisons with the present catalyst must be viewed as tentative, nevertheless there is at least a semiquantitative correspondence. The ammonium 12-tungstophosphate has weaker acidic sites and quite possibly a broader distribution of acid strengths than its parent acid. While the 12-tungstophosphoric acid is more prone to the production of carbon and olefinic species, its ammonium salt produces less coke and primarily paraffinic product. Evidently hydrogen transfer occurs more readily with the salt than with the acid.

It is important to present some comments, however hypothetical, concerning the source of the differences between the ammonium salt and its parent free acid. It has been shown (*3a*) that chemisorption of ammonia on the free acid increases neither the activity nor the selectivity in the methanol conversion process. The X-ray diffraction data display structural differences between the salt and its acid. Analytical data show that little or no nitrogen is lost from the ammonium salt with pretreatment to 500°C and with subsequent exposures to methanol at 400°C. In addition, the surface area of the ammonium salt is considerably larger than that of the acid. Thus there are not only structural differences between the salt and the acid but in addition the ammonium ion appears to be relatively tightly bound with no evidence for the loss of ammonia at elevated temperatures. The major alteration which has occurred in converting the acid to the salt must presumably be found in the elimination of acidic protons representing a relatively narrow distribution of acidic strengths or the modification of these protons to produce a shift in the acidic strength distribution.

Brown *et al.* (*25*) have concluded, from single-crystal X-ray and neutron diffraction data for the hexahydrate of 12-tungstophosphoric acid, that the anions ($PW_{12}O_{40}^{3-}$) are interconnected by $H_5O_2^+$ cations (Fig. 11), through hydrogen bonding of the hydrogen atoms of the water molecules to the oxygen atoms of the anions. Brown *et al.* (*25*) find that the oxygen atoms of the water molecules are arranged in squares of dimension 1.676 Å (Fig. 12) with one of the protons of the acid at the center of each square. Although there are four water molecules cen-

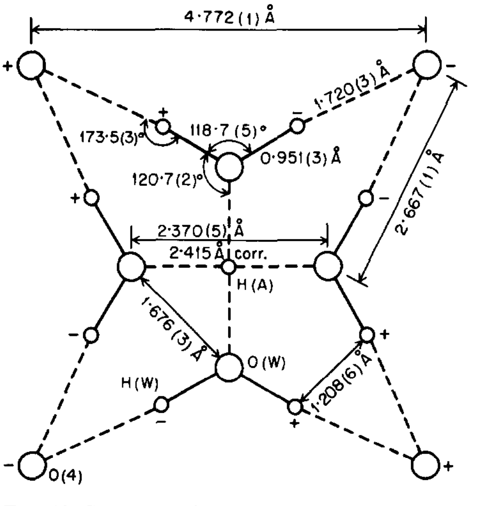

FIG. 12. Structure of the diaquahydrogen ion $H_5O_2^+$ and its hydrogen-bonding to oxygen atoms of the Keggin units. Reproduced, with permission, from (*25*).

tered around the proton, only one $H_5O_2^+$ ion exists at the site, but with two possible orientations (Fig. 12). Brown *et al.* (*25*) note that the structure may be considered as made up of two different interpenetrating substructures of anions and disordered $H_5O_2^+$ cations with no hydrogen-bonding between these two substructures.

In the absence of detailed information on the structure of the ammonium salt of 12-tungstophosphoric acid, discussion will be based on the qualitative features of that for the acid. The distance between the proton and one of the oxygen atoms of the anion (Fig. 12) is approximately 3.38 Å in the acid. The evidence from the present work suggests that the nitrogen is retained at a temperature 100° higher than that at which all the water is eliminated from the ammonium salt. The catalyst as employed in the present work should apparently be considered, at the reaction temperatures, as resulting from the replacement of both the water molecules and the protons by the ammonium ion. One or more of the hydrogen atoms of the ammonia molecule may hydrogen-bond to the oxygen atoms of the anion. This would then produce a hydrogen bond approximately 2.4 Å in length, in contrast with the values of 1.2 and 1.7 Å found for H_2O --- H^+ and HOH --- O found by Brown *et al.* (*25*). It is to be expected that the cation cavity would decrease in volume, that is, the cation–cation separations must decrease to minimize the energy associated with the overall structure. The protonic acidity can then be associated with the ionization constant of the ammonium ion ($K_a = 5.6 \times 10^{-10}$ at 25°C) which is a considerably weaker acid than the heteropoly acid itself (*1*, *2*).

The methanol conversion process may then be visualized as one in which the dimethyl ester becomes initially hydrogen-bonded with an ammonium hydrogen.

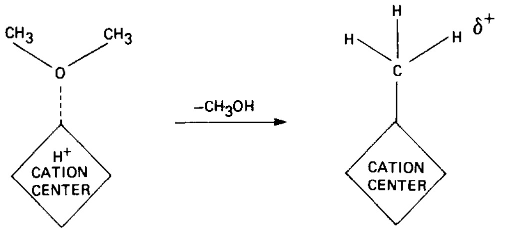

Subsequent interaction between the new surface species and a further ether molecule may lengthen the hydrocarbon chain:

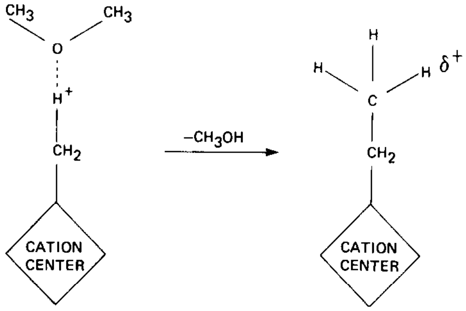

The hydrocarbon chain may be further lengthened by continued operation of process (3) or by the desorption of the carbonium ion formed on the surface.

ACKNOWLEDGMENT

The financial support of the Natural Sciences and Engineering Research Council through a Strategic Grant is gratefully acknowledged. The authors are pleased to thank H. Grisebach for his technical assistance.

REFERENCES

1. Tsigdinos, G. A., *in* "Methodicum Chimicum" (F. Korte, Ed.), Vol. 8, Chap. 32, Academic Press, New York, 1976.
2. Tsigdinos, G. A., *Top. Curr. Chem.* **76,** 1 (1978).
3. (a) Hayashi, H., and Moffat, J. B., *J. Catal.* **77,** 473 (1982); (b) Hayashi, H., and Moffat, J. B., *Talanta* **29,** 943 (1982); (c) Hayashi, H., and Moffat, J. B., *J. Catal.* **81,** 61 (1983).
4. Furuta, M., Sakata, K., Misono, M., and Yoneda, Y., *Chem. Lett.*, 31 (1979).
5. Eguchi, K., Aso, I., Yamazoe, N., and Seiyama, T., *Chem. Lett.*, 1345 (1979).
6. Ai, M., *J. Catal.* **67,** 110 (1981).
7. Ai, M., *J. Catal.* **71,** 88 (1981).

8. Knoth, W. H., and Harlow, R. L., *J. Amer. Chem. Soc.* **103,** 4265 (1981).
9. Akimoto, M., Tsuchida, Y., Sato, K., and Echigoya, E., *J. Catal.* **72,** 83 (1981).
10. Baba, T., Sakai, J., Ono, Y., and Keii, T., 47th Meeting of Catalysis Society of Japan; *Shokubai Catal.* **23,** 108 (1981).
11. Ono, Y., Baba, T., Sakai, J., and Keii, T., *J. Chem. Soc. Chem. Commun.*, 400 (1981).
12. Kasai, A., Okuhara, T., Misono, M., and Yoneda, Y., *Chem. Lett.*, 449 (1981).
13. Hall, W. K., Leftin, H. A., Cheselske, F. J., and O'Reilly, D. E., *J. Catal.* **2,** 506 (1963).
14. Hall, W. K., Wallace, W. E., and Cheselske, F. J., *J. Phys. Chem.* **65,** 128 (1961).
15. Moffat, J. B., and Scott, L. G., *J. Catal.* **45,** 310 (1976).
16. van Hooff, J. H. C., *in* "Chemistry and Chemical Engineering of Catalytic Processes," (R. Prins and G. C. A. Schuit, Eds.), p. 615, Sijthoff & Noordhoff, 1980.
17. Bailey, Wm. A., Jr., and Sartor, A. F., *Adv. Pet. Chem. Refin.* **5,** 228 (1962); Wiley, New York.
18. Greensfelder, B. S., and Voge, H. H., *Ind. Eng. Chem.* **37** (514), 983 (1945).
19. Greensfelder, B. S., Voge, H. H., and Good, G. M., *Ind. Eng. Chem.* **41,** 2573 (1949).
20. Rossini, F. D., *in* "Physical Chemistry of Hydrocarbons" (A. Farkas, Ed.), Vol. 1, Academic Press, New York, 1953.
21. Chang, C. D., and Silvestri, A. J., *J. Catal.* **47,** 249 (1977).
22. Otouma, H., Arai, Y., and Ukihashi, H., *Bull. Chem. Soc. Japan* **42,** 2449 (1969).
23. Eastwood, S. C., Planck, C. J., and Weisz, P. B., Proceedings, 8th World Petrol. Congress, Moscow, 1971.
24. Weisz, P. B., "Chemtech," p. 498, Aug. 1973.
25. Brown, G. M., Noe-Spirlet, M.-R., Busing, W. R., and Levy, H. A., *Acta Crystallogr. Sect. B* **33,** 1038 (1977).